
Tile2Vec: Unsupervised representation learning for remote sensing data

Neal Jean
Stanford University
nealjean@stanford.edu

Sherrie Wang
Stanford University
sherwang@stanford.edu

George Azzari
Stanford University
gazzari@stanford.edu

David Lobell
Stanford University
dlobell@stanford.edu

Stefano Ermon
Stanford University
ermon@stanford.edu

Abstract

Remote sensing lacks methods like the word vector representations and pre-trained networks that significantly boost performance across a wide range of natural language and computer vision tasks. To fill this gap, we introduce Tile2Vec, an unsupervised representation learning algorithm that extends the distributional hypothesis from natural language — words appearing in similar contexts tend to have similar meanings — to geospatial data. We demonstrate empirically that Tile2Vec learns semantically meaningful representations on three datasets. Our learned representations significantly improve performance in downstream classification tasks and similarly to word vectors, visual analogies can be obtained by simple arithmetic in the latent space.

1 Introduction

Remote sensing, the measurement of the Earth’s surface through aircraft- or satellite-based sensors, is becoming increasingly important to applications from sustainability and developmental economics to precision agriculture and military intelligence [5, 19, 15]. Several features of remotely-gathered data make it attractive for large-scale analysis:

- *Low marginal cost*: Traditional data collection methods, e.g., a national census, are extremely expensive, while remote sensing is characterized by low marginal costs.
- *Accessibility*: Some areas of the world are dangerous or hard to reach, e.g., tracking refugees in conflict regions or deforestation in the Amazon.
- *Real-time monitoring*: Many tasks demand continuous monitoring that is unrealistic to maintain on the ground but possible through satellites or aircraft with high revisit rates.
- *Global coverage*: The United Nations hopes to track 169 metrics in every country to measure progress towards the Sustainable Development Goals (SDGs) — remote sensing is perhaps the only regularly updated and consistently calibrated source of data with global coverage.

Combined with recent advances in deep learning and computer vision [11, 9], there is enormous potential for monitoring global issues through the automated analysis of remote sensing data streams. However, recent successes in machine learning have largely relied on supervised learning techniques and the availability of very large annotated datasets. Remote sensing provides a huge supply of data, but for many tasks that we would like to tackle, we are constrained by a lack of labels. Whether we are trying to predict crop yields in Africa [2] or poverty in Sri Lanka [4], we often have limited quantities of labeled data — or none at all — on which to train models end-to-end.

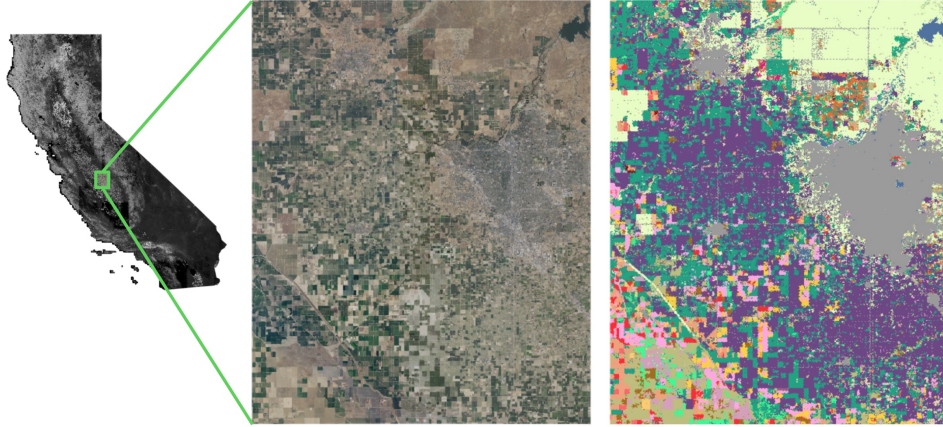


Figure 1: Aerial imagery downloaded from the National Agriculture Imagery Program (NAIP) through Google Earth Engine. (Left) Our 50 GB dataset of a section of Central Valley covers a roughly 2500 km^2 area surrounding Fresno, California and contains over 12 billion multispectral pixels. (Center) The image consists of red, green, blue, and infrared color bands at 0.6 m ground resolution. (Right) Land cover types in the region as labeled by the Cropland Data Layer (CDL, see Section 3.4) show a highly heterogeneous landscape; each color represents a different CDL class.

The research community has developed a number of unsupervised and semi-supervised learning techniques to mitigate the need for labeled data. Often, the key underlying idea is to find a low-dimensional *representation* of the data that is more suitable for downstream machine learning tasks. For example, in many NLP applications, the use of pre-trained word vectors often leads to dramatic performance improvements. In computer vision, pre-training on ImageNet is a *de facto* standard that can drastically reduce the amount of training data needed for new tasks. Existing techniques, however, are not suitable for remote sensing data. While on the surface they may resemble natural images, remote sensing data have unique characteristics that require new methodologies.

In this paper, we fill this gap by proposing a new approach for learning compressed yet highly informative representations of remote sensing data. Unlike natural images, which are object-centric, two-dimensional depictions of three-dimensional scenes, remote sensing images are taken from a bird’s eye perspective and also often *multi-spectral*. This presents both challenges and opportunities. On one hand, models pre-trained on ImageNet do not perform well and cannot take advantage of additional bands beyond RGB. On the other, there are few occlusions in satellite images: instead of objects at different depths blocking things behind them, objects seen in satellite images are usually continuous and viewed in full. This simple property of spatial coherence provides a powerful signal for learning image representations.

Our main assumption is that image patches that are geographic neighbors (close spatially) should have similar semantics and therefore representations, while tiles far apart are likely to have dissimilar semantics and should therefore have dissimilar representations. This is akin to the *distributional hypothesis* used to construct word vector representations in natural language: words that appear in similar contexts should have similar meanings. The main computational (and statistical) challenge is that image patches are themselves complex, high-dimensional vectors (unlike words) — again, standard approaches cannot be applied.

To overcome this challenge we propose Tile2Vec, an unsupervised method for learning useful latent representations from unlabeled remote sensing data. We evaluate our algorithm on a wide range of remote sensing data sources and find that it generalizes to all of these data modalities, with stable training and robustness to hyperparameter choices. On a difficult land use classification task, these Tile2Vec representations outperform other unsupervised features and can surprisingly even exceed the performance of supervised models trained on large labeled training sets. Our learned representations also comprise a meaningful embedding space — through visual query by example and visual analogy experiments, we show that high-level semantic features can be learned without supervision.

2 Tile2Vec

We first motivate *Tile2Vec* and provide some intuition, and then describe in detail the algorithm and training procedure.

2.1 Distributional semantics

The distributional hypothesis in linguistics refers to the idea that “a word is characterized by the company it keeps”. In natural language processing, algorithms like Word2vec and GloVe leverage this assumption to learn continuous representations that capture the nuanced meanings of huge vocabularies of words. The strategy is to build a co-occurrence matrix and then compute or learn a low rank approximation in which words that appear in similar contexts have similar vector representations [13, 24, 17].

To extend these ideas to the distributional semantics of remote sensing data, we need to answer the following questions:

- What is the right atomic unit, i.e., the equivalent of individual words in NLP?
- What is the right notion of context?

For atomic units, we propose to learn representations at the level of remote sensing *tiles*, a generalization of image patches to multi-spectral data. This already introduces new challenges, as tiles are themselves high-dimensional objects — computations on co-occurrence matrices of tiles would quickly become intractable, and statistics almost impossible to estimate from finite data. As we have come to expect, convolutional neural networks (CNNs) will be crucial in projecting down the dimensionality of our inputs.

For context, we will rely on spatial *neighborhoods*. Distance in geographical space provides a form of weak supervision: we assume that tiles that are close together have similar semantics and therefore should, on average, have more similar representations than tiles that are far apart. By exploiting this fact that landscapes in remote sensing datasets are highly spatially correlated, we hope to extract enough learning signal to reliably train deep neural networks.

2.2 Unsupervised triplet loss

To learn a mapping from image tiles to low-dimensional embeddings, we train a convolutional neural network on triplets of tiles, where each triplet consists of an anchor tile t_a , a neighbor tile t_n that is close geographically, and a distant tile t_d that is farther away. Following our distributional assumption, we want to minimize the Euclidean distance between the embeddings of the anchor tile and the neighbor tile, while maximizing the distance between the anchor and distant embeddings. For each tile triplet (t_a, t_n, t_d) , we seek to minimize the triplet loss

$$L(t_a, t_n, t_d) = [\|f_\theta(t_a) - f_\theta(t_n)\|_2 - \|f_\theta(t_a) - f_\theta(t_d)\|_2 + m]_+ \quad (1)$$

To prevent the network from pushing the distant tile farther without restriction, we introduce a rectifier with margin m : once the distance to the distant embedding is greater than the distance to the neighbor embedding by at least the margin, we are satisfied. Here, f_θ is a CNN with parameters θ that maps from the domain of image tiles \mathcal{X} to d -dimensional real-valued vector representations, $f_\theta : \mathcal{X} \rightarrow \mathbb{R}^d$.

Notice that when $\|f_\theta(t_a) - f_\theta(t_n)\|_2 < \|f_\theta(t_a) - f_\theta(t_d)\|_2$, all embeddings can be scaled by some constant in order to satisfy the margin and bring the loss to zero. We observe this behavior empirically: beyond a small number of iterations, the CNN learns to increase embedding magnitudes and the loss decreases to zero. By penalizing the embeddings’ l^2 -norm, we constrain the network to generate embeddings within a hypersphere, leading to a representation space in which relative distances have meaning. Given a dataset of N tile triplets, our full training objective is

$$\min_{\theta} \sum_{i=1}^N \left[L(t_a^{(i)}, t_n^{(i)}, t_d^{(i)}) + \lambda \left(\|z_a^{(i)}\|_2 + \|z_n^{(i)}\|_2 + \|z_d^{(i)}\|_2 \right) \right], \quad (2)$$

where $z_a^{(i)} = f_\theta(t_a^{(i)}) \in \mathbb{R}^d$ and similarly for $z_n^{(i)}$ and $z_d^{(i)}$.

Algorithm 1 SampleTileTriplets(D, N, s, r)

```
1: Input: Image dataset  $D$ , number of triplets  $N$ , tile size  $s$ ,  
   neighborhood radius  $r$   
2: Output: Tile triplets  $T = \{(t_a^{(i)}, t_n^{(i)}, t_d^{(i)})\}_{i=1}^N$   
3:  
4: Initialize tile triplets  $T = \{\}$   
5: for  $i \leftarrow 1, N$  do  
6:    $t_a^{(i)} \leftarrow \text{SAMPLETILE}(D, s)$   
7:    $t_n^{(i)} \leftarrow \text{SAMPLETILE}(\text{NEIGHBORHOOD}(D, r, t_a^{(i)}), s)$   
8:    $t_d^{(i)} \leftarrow \text{SAMPLETILE}(\neg\text{NEIGHBORHOOD}(D, r, t_a^{(i)}), s)$   
9:   Update  $T \leftarrow (t_a^{(i)}, t_n^{(i)}, t_d^{(i)})$   
10: end for  
11: return  $T$   
12:  
13: function SAMPLETILE( $A, s$ )  
14:    $t \leftarrow$  Sample tile of size  $s$  uniformly at random from  $A$   
15:   return  $t$   
16: end function  
17:  
18: function NEIGHBORHOOD( $D, r, t$ )  
19:    $A \leftarrow$  Subset of  $D$  within radius  $r$  of tile  $t$   
20:   return  $A$   
21: end function
```

2.3 Triplet sampling

The sampling procedure for t_a , t_n , and t_d is described by two parameters:

- **Tile size** defines the pixel width and height of a single tile.
- **Neighborhood radius** defines the box around the anchor tile from which to sample the neighbor tile. E.g., if the neighborhood is 100 pixels, then the center pixel of the neighbor tile must be within 100 pixels of the anchor tile center pixel both vertically and horizontally.

The choice of these parameters should depend on the dataset, but we provide some heuristic guidance here. Tile size should be chosen so that tiles are large enough to contain information at the scale needed for downstream tasks. Neighborhood radius should be small enough that neighbor tiles will be semantically similar to the anchor tile, but large enough to capture intra-class (and potentially some inter-class) variability. In practice, we find that plotting some example triplets as in Fig. 4 allowed us to easily find reasonable values for these parameters. Pseudocode for sampling a dataset of triplets is given in Algorithm 1. Note that no knowledge of actual geographical locations is needed, so Tile2Vec can be applied to any dataset without knowledge of the data collection procedure.

2.4 Scalability

Like most deep learning algorithms, the Tile2Vec objective (Eq. 2) allows for mini-batch training on large datasets. More importantly, the use of the triplet loss allows the training dataset to grow with a *power law* relationship relative to the size of the available remote sensing data.

Concretely, assume that for a given remote sensing dataset we have a sampling budget of N triplets, imposed perhaps by storage constraints. If we train using the straightforward approach of Eq. 2, we will iterate over N training examples in each epoch. However, we notice that in most cases the area covered by our dataset is much larger than the area of a single neighborhood. For any tile t , the likelihood that any particular t' in the other $(N - 1)$ tiles is in its neighborhood is extremely low. Therefore, at training time we can match any (t_a, t_n) pair with any of the $3N$ tiles in the dataset to massively increase the number of unique example triplets that the network sees from $\mathcal{O}(N)$ to $\mathcal{O}(N^2)$.

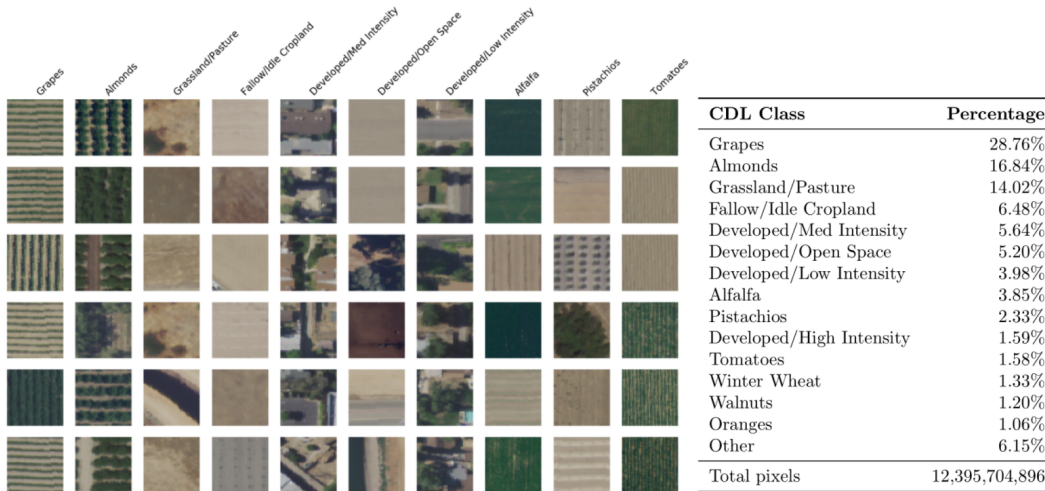


Figure 2: Six random examples of 50-by-50 pixel (30-by-30 m) tiles sampled from NAIP imagery. The top 10 classes in CDL (Section 3.4) are shown, with grapes being the most common. We label a tile with a CDL class if more than 80% of pixels in the tile are in said class. There are 57 CDL classes in our entire dataset; the top 10 classes account for 88% of tiles. Note the high within-class variability of tiles relative to between-class variability, which makes CDL classification a difficult task.

In practice, we find that combining Tile2Vec with this data augmentation scheme to create massive datasets results in an algorithm that is easy to train, robust to hyperparameter choices, and resistant to overfitting. This point will be revisited in section 4.1.5.

3 Data

We test Tile2Vec on three classes of widely used imagery with varying characteristics (e.g., satellite vs. aerial, resolution, spectral range). In this section, we describe the datasets that we use, explain how we sample our training data, and provide summary statistics and other high-level analysis.

3.1 NAIP

We obtain a large static aerial image from the National Agriculture Imagery Program (NAIP) of Central Valley, California near the city of Fresno for the year 2016 (Fig. 1). The image spans latitudes $[36.45, 37.05]$ and longitudes $[-120.25, -119.65]$. The study area contains a mixture of urban, suburban, agricultural, and other land use types; it was chosen for this diversity of land cover, which makes for a difficult classification task.

The NAIP imagery consists of four spectral bands — red (R), green (G), blue (B), and infrared (N) — at 0.6 m ground resolution. Images of the study area amount to a 50 GB dataset containing over 12 billion multi-spectral pixels, and were exported piece-wise using Google Earth Engine [8]. NAIP is an ideal remote sensing dataset in many ways: it is publicly accessible, has only cloud-free images, and its 0.6 m resolution allows a CNN to learn features (individual plants, small buildings, etc.) helpful for distinguishing land cover types that are only visible at high resolution.

3.2 DigitalGlobe

DigitalGlobe is a company that provides high-resolution satellite data and supplies much of the imagery for Google Maps and Google Earth. Image samples from a global composite with up to 0.3 m resolution are available free of charge through the Google Static Maps API.¹

¹<https://developers.google.com/maps/documentation/static-maps/>



Figure 3: Landsat 8 median composites of three major US cities downloaded through Google Earth Engine: (Left) San Francisco, (Center) New York City, and (Right) Boston.

We sample a dataset of 11,564 satellite images tiling the area surrounding Addis Ababa, Ethiopia and spanning latitudes [8.86, 9.15] and longitudes [38.62, 38.91]. This dataset contains roughly 2.9 billion RGB pixels at zoom level 18, roughly corresponding to 0.6 m resolution.

3.3 Landsat 8

The Landsat satellites are a series of Earth-observing satellites jointly managed by the USGS and NASA. Landsat 8 provides moderate-resolution (30 m) satellite imagery in seven surface reflectance bands: ultra blue, blue, green, red, near infrared, shortwave infrared 1, and shortwave infrared 2 [27]. The spectral bands were designed to serve a wide range of scientific applications, from estimating vegetation biophysical properties to monitoring glacial runoff. Near-infrared and shortwave-infrared regions of the electromagnetic spectrum can capture ground properties that are difficult to see in the visible bands alone. For this reason, they are effective features in separating different land cover types, and often play a key role in classic, pixel-level supervised classification problems.

Landsat images are collected on a 16-day cycle and often affected by different type of contamination, such as clouds, snow, and shadows [30]. Although contaminated pixels can be removed using masks that are delivered with the images, it can be challenging to obtain a completely clear image over large areas without human supervision. Remote sensing scientists often solve this problem by generating pixel-level composites of several images [14].

In this study, we generate and export median composites over three major US cities and their surrounding area: San Francisco, New York City, and Boston. Each image spans 1.2 degrees latitude and longitude and contains just under 20 million pixels.

3.4 Cropland Data Layer (CDL)

The Cropland Data Layer (CDL) is a raster geo-referenced land cover map collected by the USDA for the entire continental United States [1]. It is offered at 30 m resolution and includes 132 detailed class labels spanning field crops, tree crops, developed areas, forest, water, and more. In our dataset of Central Valley, we observe 57 CDL classes (Fig. 2).

In this paper, we treat CDL labels as ground truth and use them to evaluate the quality of features learned by various unsupervised and supervised methods. To do this, we upsample CDL to NAIP resolution in Google Earth Engine, allowing us to assign every NAIP pixel a CDL class. CDL is created yearly using imagery from Landsat 8 and the Disaster Monitoring Constellation (DMC) satellites, and a decision tree algorithm trained and validated on ground samples. Our evaluation accuracies depend on the quality of the CDL labels themselves, which vary by class — for the most common classes, accuracies detailed in the CDL metadata generally exceed 90%.

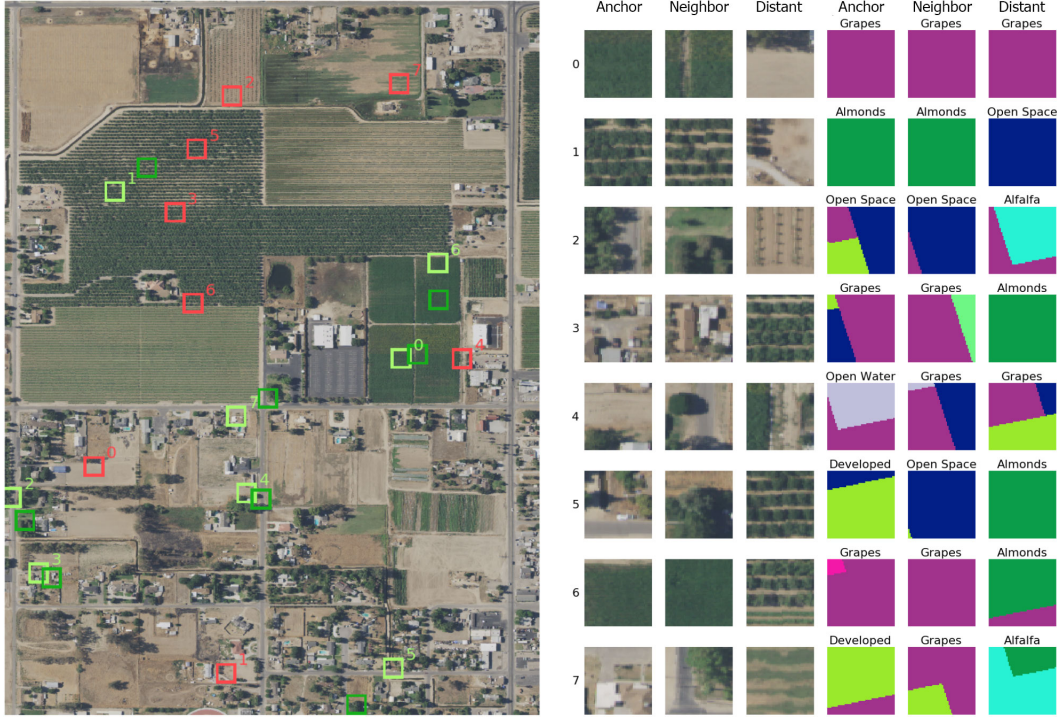


Figure 4: Eight example triplets sampled at random from a section of our NAIP dataset to illustrate the sampling methodology. (Left) Light green boxes encircle anchor tiles, dark green neighbor tiles, and red distant tiles. The three tiles with the same ID are embedded by the model and used to calculate triplet loss. Neighbor tiles are sampled from within 100 pixels of the anchor center and distant tiles from outside this area. (Right) Tile triplets in order of IDs corresponding to those shown in the left panel. The first, second, and third columns show the anchor, neighbor, and distant tiles, respectively. The fourth, fifth, and sixth columns show CDL labels for the triplet. Anchor and neighbor tiles tend to come from the same CDL class, while anchor and distant tiles tend to come from different CDL classes; this provides the signal for our unsupervised learning algorithm.

4 Experiments

In all experiments across all datasets, we use 50×50 tiles and 100 pixel neighborhoods for our Tile2Vec embeddings. For our Tile2Vec CNN, we use a ResNet-18 architecture [9] adapted for 28×28 CIFAR-10 images and add an additional residual block to handle our larger input — to avoid confusion, we will continue to refer to this model as ResNet-18. For Tile2Vec embeddings, we remove the final classification layer; for supervised experiments, we change the number of output classes to 57 to match our CDL dataset. Experimental results are organized by remote sensing dataset.

4.1 NAIP: Land use classification

4.1.1 Overview

We train Tile2Vec embeddings on 100k tile triplets sampled from the NAIP dataset from Central Valley California. Each of the 300k 50×50 NAIP tiles is labeled with the majority CDL land use class if the majority class makes up over 80% of the pixels — this results in a labeled dataset of 232,262 tiles for evaluation on the downstream classification task. Our metric for comparison is accuracy on CDL label classification.

Unsupervised features	Accuracy (%)	
	$n = 1000$	$n = 10000$
Tile2Vec	65.5 ± 2.5	72.2 ± 0.8
Pre-trained ResNet-18	60.8 ± 2.9	63.5 ± 1.3
PCA	58.2 ± 5.0	62.8 ± 1.2
ICA	58.7 ± 3.6	62.7 ± 1.1
Autoencoder	52.3 ± 2.2	57.1 ± 0.9
K-Means	53.8 ± 2.9	56.8 ± 1.3

Table 1: Performance comparison of Tile2Vec features against unsupervised baselines on the CDL classification task described in Section 4.1. Random forest classifiers are trained using each type of features over 10 trials of $n = 1000$ and $n = 10000$ randomly sampled labels. Baselines are described in detail in Section 4.1.2.

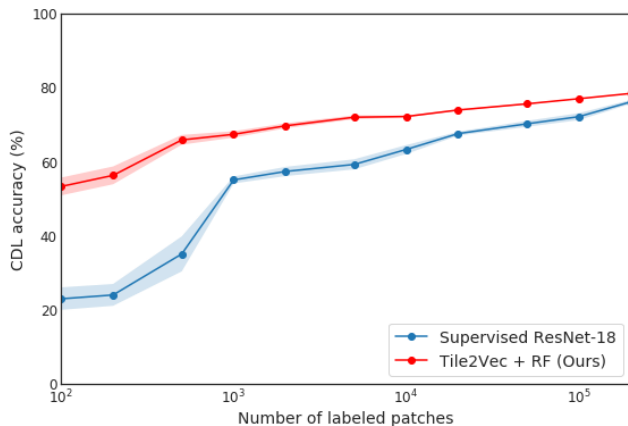


Figure 5: Training a random forest on Tile2Vec unsupervised features outperforms a supervised ResNet with as many as 200k labeled image tiles. The Tile2Vec CNN and the supervised ResNet share the same architecture up to the final classification layer, which is removed for the Tile2Vec CNN. Given more labels, we expect that the supervised approach will eventually outperform — however, the 230k labeled tiles in our NAIP dataset is not enough.

4.1.2 Unsupervised baselines

We compare Tile2Vec to a number of other unsupervised feature extraction methods. The features obtained by unsupervised methods are used as input to a random forest to perform land cover classification. We describe each baseline here, and provide additional training details in Appendix A.

- **PCA/ICA:** Each RGBN tile of shape $(50, 50, 4)$ is unraveled into a vector of length 10,000 and then PCA/ICA is used to extract the first $n = 10$ principal components for each tile.
- **K-means:** We cluster the tiles in pixel space using k-means with $k = 10$, and then represent each tile as 10-dimensional vectors of their distances to each cluster centroid.
- **Pre-trained ResNet-18:** We train our modified ResNet-18 on resized CIFAR-10 images and used this pre-trained network as a feature extractor. Since CIFAR-10 only has RGB channels, this approach only allows for use of the RGB bands of NAIP; it is unable to take advantage of the infrared frequency band.
- **Autoencoder:** We train a convolutional autoencoder on all 300k NAIP tiles, splitting them 90% training and 10% validation. Training is performed until the validation reconstruction error stopped decreasing; the trained encoder is then used to embed tiles into the feature space. We train on the full multi-spectral tiles, with RGB and infrared channels.

As shown in Table 1, the features learned by Tile2Vec easily outperform other unsupervised features when used by a random forest trained on $n = 1000$ or $n = 10000$ labels. Recent improvements

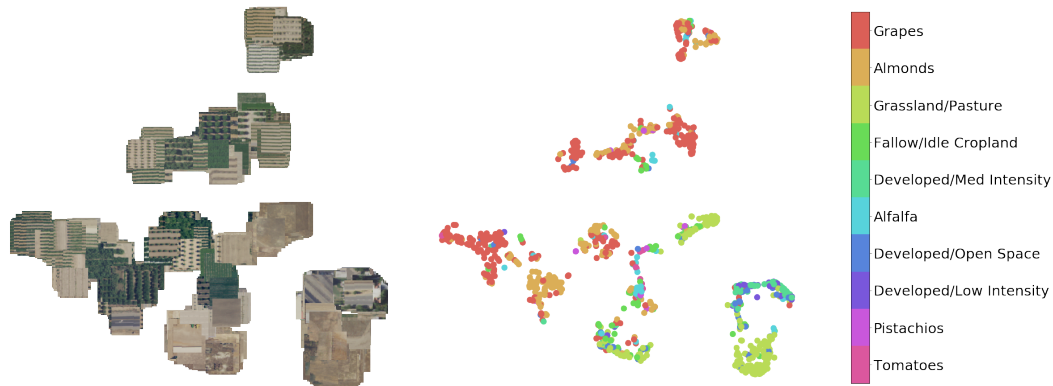


Figure 6: (Left) NAIP image tiles visualized with t-SNE in the Tile2Vec learned embedding space. (Right) The same learned embeddings for tiles represented as colored points where the colors correspond to the CDL label for each tile. Only the top 10 most common CDL classes are shown for clarity.

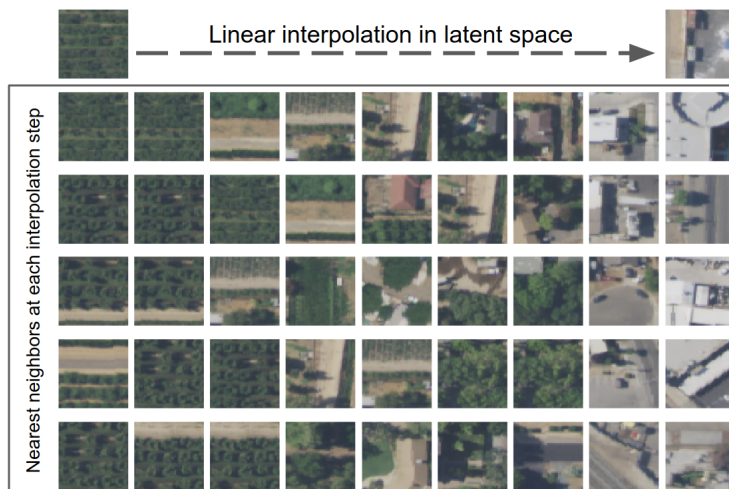


Figure 7: Linear interpolation in the latent space learned by Tile2Vec demonstrates that the representations are semantically meaningful. In this example, we interpolate linearly at equal intervals between the Tile2Vec representations of the farm and urban images in the top row. Below, we show the five nearest neighbors to each interpolated vector in the latent space.

in generative models of images based on generative adversarial networks (GANs) and variational autoencoders (VAEs) would also provide intriguing baselines, but we are unaware of any current models that are capable of capturing complex multi-spectral image distributions.

4.1.3 Supervised comparison

Surprisingly, our Tile2Vec features are also able to outperform a fully-supervised deep neural network trained directly on the downstream task with large amounts of labeled data. In Fig. 5, we see that applying a random forest on Tile2Vec features, which are trained without supervision, beats a supervised ResNet-18 trained on as many as 200k CDL labels. We emphasize that the Tile2Vec CNN and the supervised ResNet-18 share the same architecture up to the final classification layer, which is removed for the Tile2Vec CNN. We expect that with more labeled training data, the end-to-end supervised approach will eventually outperform Tile2Vec. However, our NAIP dataset contains only 230k labeled tiles — not enough for the supervised ResNet-18 to fully close the gap.

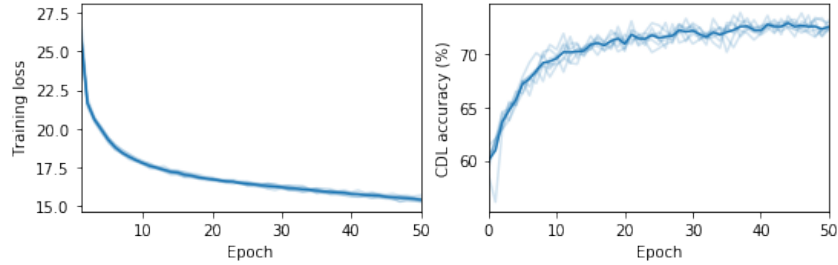


Figure 8: Training loss and CDL accuracy per epoch over 10 trials. Note that the consistent decrease in the unsupervised training loss (left) leads to a corresponding increase in performance on the downstream task of interest (right). Each epoch represents 100k triplets; even after training for many epochs we don’t observe any overfitting.

4.1.4 Learned representations

Fig. 6 shows how the learned Tile2Vec embedding clusters tiles from the same CDL class together in the latent space. Note that some classes have multiple clusters — recall the high intra-class variability seen in Fig. 2. Some crops may look similar to other crops depending on when in the growing season the images are taken, how old the plants are, and many other reasons. For the CDL classification task, we want to learn a representation that clusters different crop types; for other potential downstream tasks, we may want a different clustering. Being unsupervised, Tile2Vec is agnostic to the downstream application and learns a representation that obeys the distributional semantics of the image dataset.

We further explore the learned representations with a latent space interpolation experiment shown in Fig. 7. Here, we start with the Tile2Vec embeddings of a field tile and an urban tile and linearly interpolate between the two. At each point along the interpolation, we search for the five nearest neighbors in the latent space and plot the corresponding tiles. As we move through the semantically meaningful latent space, we recover tiles that are more and more developed.

4.1.5 Training details

Unlike many state-of-the-art deep learning models, Tile2Vec is easy to train and robust to the choice of hyperparameters. For the NAIP/CDL classification task, we experimented with margins ranging from 0.1 to 100 and found that accuracy on the downstream task never dropped below 67-68% for $n = 10000$. Using a margin of 50, we trained Tile2Vec for 10 trials with different random initializations and show the results in Fig. 8. We note that the loss is extremely stable from epoch to epoch and consistently decreasing. More importantly, the training loss is a good proxy for unsupervised feature quality as measured by performance on the downstream task.

Tile2Vec is able to learn good features even without regularizing the magnitudes of the learned embeddings (Eq. 2), with performance around 68%. However, by combining explicit regularization with the data augmentation scheme described in Section 2.4, we observe that Tile2Vec does not seem overfit even when trained for many epochs.

4.2 DigitalGlobe: Visual query by example

Next we train a Tile2Vec model on DigitalGlobe image tiles from Addis Ababa, Ethiopia to explore whether the model generalizes (1) to multiple modes of imaging (satellite vs. aerial) and (2) to very different landscapes (sub-Saharan Africa vs. Central Valley California). We also want to test the model in the developing world, where there is very little labeled data — unsupervised methods for remote sensing could enable monitoring of infrastructure development and other humanitarian goals.

In Fig. 9, we show that the latent representations learned by Tile2Vec allow us to do visual query by example: given a starting location, we can search for neighbors in the latent space to find other similar locations. This type of visual query has previously been explored in the supervised setting [12], and has applications from military reconnaissance to disaster recovery.

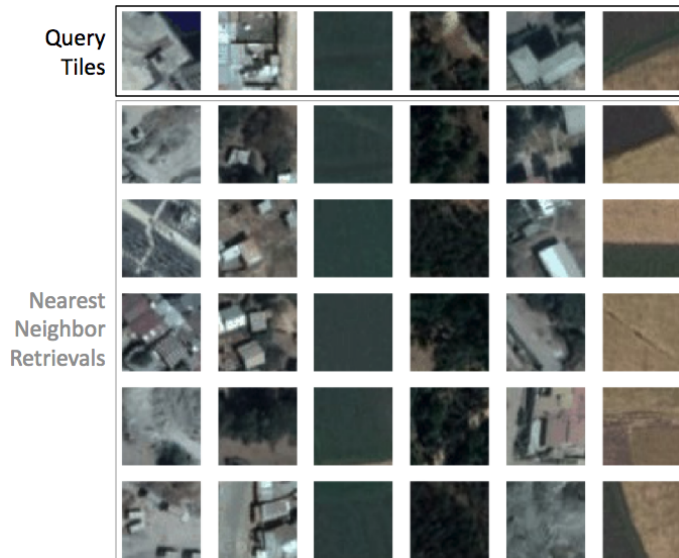


Figure 9: Visual query by example in Addis Ababa, Ethiopia. The top tile in each column is the query; its five nearest neighbors in the embedding space fill the rest of the column.

4.3 Landsat 8: Visual analogies

In our final experiment, we explore the application of Tile2Vec to three major metropolitan areas of the United States: San Francisco, New York City, and Boston.

First, we train a Tile2Vec model on the San Francisco dataset only. Then we use the trained model to embed tiles from all three cities. As shown in Fig. 10, these learned representations allow us to perform simple arithmetic in the latent space, or visual analogies [25]. By adding and subtracting vectors in the latent space, we can recover image tiles that are semantically what we would expect given the operations applied.

From this experiment, we conclude that Tile2Vec can be applied effectively to highly multi-spectral datasets, as we use the full Landsat images with 7 spectral bands. Tile2Vec is also able to learn representations at multiple scales: Landsat 8 is at 30 m resolution so each tile covers a 2.25 km² area, while the NAIP and DigitalGlobe tiles are 2500 times smaller. Finally, we observe that Tile2Vec learns robust representations that allow for domain adaptation or transfer learning. In Fig. 3, we see that the San Francisco dataset has a much different spectral distribution than that of the New York or Boston datasets, yet we are able to apply the model trained only on San Francisco data successfully in both of the other cities.

5 Related Work

Our inspiration for using spatial context to learn representations originated from continuous word representations like Word2vec and GloVe [17, 16, 24]. In NLP, the distributional hypothesis can be summarized as “a word is characterized by the company it keeps” — words that appear in the same context likely have similar semantics. We apply this concept to remote sensing data, with multi-spectral image tiles as the atomic unit analogous to individual words in NLP, and geospatial neighborhoods as the “company” that these tiles keep.

A related, supervised version of this idea is the patch2vec algorithm [6], which its authors describe as learning “globally consistent image patch representations”. Working with natural images, they use a very similar triplet loss, but sample their patches *with supervision* from an annotated semantic segmentation dataset. This allows them to pick anchor and neighbor patches that come from the same object, and then a negative patch that is not from the same object. In the remote sensing domain, the lack of semantically segmented datasets and vast heterogeneity of landscapes precludes the use

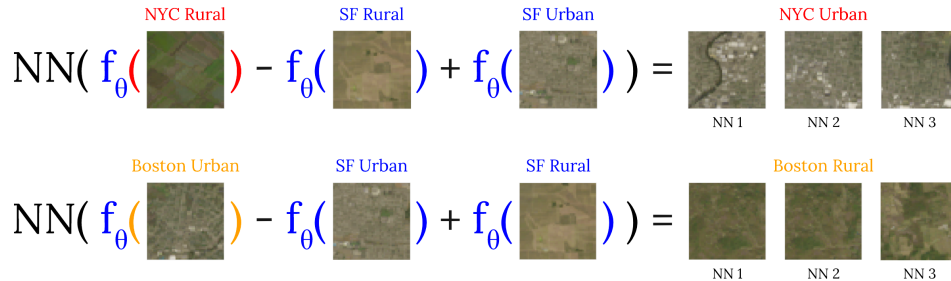


Figure 10: Visual analogies exploiting the semantically meaningful learned embedding space. In the first row, the neural network f_{θ} is trained on a dataset of images from the San Francisco (SF) metropolitan area, and then applied to a tile from a rural area near New York City (NYC), along with a rural and an urban tile from SF — the colors correspond to the datasets that the tiles come from. After the desired arithmetic is performed in the latent space, nearest neighbors retrieval on the resulting embedding returns the three closest tiles from the NYC dataset. The second row is a similar experiment, this time going from Boston Urban to Boston Rural.

of patch2vec, as the algorithm requires as input precisely the type of labels that the remote sensing community seeks to generate.

Unsupervised learning for visual data is perhaps the most active area of research in machine learning today and thus impossible to summarize concisely, but we attempt a brief overview of the most relevant topics here. The three main classes of deep generative models — likelihood-based variational autoencoders (VAEs) [10], likelihood-free generative adversarial networks (GANs) [7], and various autoregressive models [21, 28] — attempt to learn the generating data distribution from training samples.

Other related lines of work use spatial or temporal context to learn high-level image representations. Some strategies for using spatial context involve predicting the relative positions of patches sampled from within an image [20, 3] or trying to fill in missing portions of an image (in-painting) [22]. In videos, nearby frames can be used to learn temporal embeddings [26]; other methods leveraging the temporal coherence and invariances of videos for feature learning have also been proposed [18, 29].

6 Conclusion

We demonstrate the efficacy of Tile2Vec as an unsupervised feature learning algorithm for remote sensing data on tasks from land cover classification to nearest neighbor tile retrieval. Our method can be applied to datasets spanning moderate- to high-resolution, RGB-only or multi-spectral bands, and collected via aerial or satellite sensors. For equivalent quantities of labeled data, it outperforms other unsupervised feature extraction techniques on a difficult semi-supervised learning task — surprisingly, it even outperforms a supervised ResNet model trained on 200k labeled examples.

In this paper, we focus on exploiting the spatial coherence of remote sensing data, but many datasets also include sequences of images from the same locations collected over time. Temporal patterns can be highly informative for many tasks of interest (e.g., seasonality, crop planting cycles), and we plan to explore this aspect in future work. Multi-spectral imagery and remote sensing data in general have largely been neglected by the machine learning community — more research in these areas could result in enormous progress on many problems of global significance.

References

- [1] Usda national agricultural statistics service cropland data layer. published crop-specific data layer [online]., 2016.
- [2] Marshall Burke and David B Lobell. Satellite-based assessment of yield variation and its determinants in smallholder african systems. *Proceedings of the National Academy of Sciences*, 114(9):2189–2194, 2017.
- [3] Carl Doersch, Abhinav Gupta, and Alexei A Efros. Unsupervised visual representation learning by context prediction. In *Proceedings of the IEEE International Conference on Computer Vision*, pages 1422–1430, 2015.
- [4] Ryan Engstrom, David Newhouse, Vishwesh Haldavanekar, Andrew Copenhaver, and Jonathan Hersh. Evaluating the relationship between spatial and spectral features derived from high spatial resolution satellite data and urban poverty in colombo, sri lanka. In *Urban Remote Sensing Event (JURSE), 2017 Joint*, pages 1–4. IEEE, 2017.
- [5] G. M. Foody. Remote sensing of tropical forest environments: Towards the monitoring of environmental resources for sustainable development. *International Journal of Remote Sensing*, 24(20):4035–4046, 2003.
- [6] O Fried, S Avidan, and D Cohen-Or. Patch2vec: Globally consistent image patch representation. In *Computer Graphics Forum*, volume 36, pages 183–194. Wiley Online Library, 2017.
- [7] Ian Goodfellow, Jean Pouget-Abadie, Mehdi Mirza, Bing Xu, David Warde-Farley, Sherjil Ozair, Aaron Courville, and Yoshua Bengio. Generative adversarial nets. In *Advances in neural information processing systems*, pages 2672–2680, 2014.
- [8] Noel Gorelick, Matt Hancher, Mike Dixon, Simon Ilyushchenko, David Thau, and Rebecca Moore. Google Earth Engine: Planetary-scale geospatial analysis for everyone. *Remote Sensing of Environment*, pages 1–10, aug 2017.
- [9] Kaiming He, Xiangyu Zhang, Shaoqing Ren, and Jian Sun. Deep residual learning for image recognition. In *Proceedings of the IEEE conference on computer vision and pattern recognition*, pages 770–778, 2016.
- [10] Diederik P Kingma and Max Welling. Auto-encoding variational bayes. *arXiv preprint arXiv:1312.6114*, 2013.
- [11] Alex Krizhevsky, Ilya Sutskever, and Geoffrey E Hinton. Imagenet classification with deep convolutional neural networks. In *Advances in neural information processing systems*, pages 1097–1105, 2012.
- [12] G Levin, D Newbury, K McDonald, I Alvarado, A Tiwari, and M Zaheer. Terrapattern: open-ended, visual query-by-example for satellite imagery using deep learning, 2010.
- [13] Omer Levy and Yoav Goldberg. Neural word embedding as implicit matrix factorization. In *Advances in neural information processing systems*, pages 2177–2185, 2014.
- [14] W Lück and A van Niekerk. Evaluation of a rule-based compositing technique for Landsat-5 TM and Landsat-7 ETM+ images. *International Journal of Applied Earth Observation and Geoinformation*, 47:1–14, May 2016.
- [15] M. Madden, American Society for Photogrammetry, and Remote Sensing. *Manual of Geographic Information Systems*. American Society for Photogrammetry and Remote Sensing, 2009.
- [16] Tomas Mikolov, Kai Chen, Greg Corrado, and Jeffrey Dean. Efficient estimation of word representations in vector space. *arXiv preprint arXiv:1301.3781*, 2013.
- [17] Tomas Mikolov, Ilya Sutskever, Kai Chen, Greg S Corrado, and Jeff Dean. Distributed representations of words and phrases and their compositionality. In *Advances in neural information processing systems*, pages 3111–3119, 2013.
- [18] Ishan Misra, C Lawrence Zitnick, and Martial Hebert. Shuffle and learn: unsupervised learning using temporal order verification. In *European Conference on Computer Vision*, pages 527–544. Springer, 2016.
- [19] David J. Mulla. Twenty five years of remote sensing in precision agriculture: Key advances and remaining knowledge gaps. *Biosystems Engineering*, 114(4):358 – 371, 2013. Special Issue: Sensing Technologies for Sustainable Agriculture.
- [20] Mehdi Noroozi and Paolo Favaro. Unsupervised learning of visual representations by solving jigsaw puzzles. In *European Conference on Computer Vision*, pages 69–84. Springer, 2016.

- [21] Aaron van den Oord, Nal Kalchbrenner, and Koray Kavukcuoglu. Pixel recurrent neural networks. *arXiv preprint arXiv:1601.06759*, 2016.
- [22] Deepak Pathak, Philipp Krahenbuhl, Jeff Donahue, Trevor Darrell, and Alexei A Efros. Context encoders: Feature learning by inpainting. In *Proceedings of the IEEE Conference on Computer Vision and Pattern Recognition*, pages 2536–2544, 2016.
- [23] F. Pedregosa, G. Varoquaux, A. Gramfort, V. Michel, B. Thirion, O. Grisel, M. Blondel, P. Prettenhofer, R. Weiss, V. Dubourg, J. Vanderplas, A. Passos, D. Cournapeau, M. Brucher, M. Perrot, and E. Duchesnay. Scikit-learn: Machine learning in Python. *Journal of Machine Learning Research*, 12:2825–2830, 2011.
- [24] Jeffrey Pennington, Richard Socher, and Christopher Manning. Glove: Global vectors for word representation. In *Proceedings of the 2014 conference on empirical methods in natural language processing (EMNLP)*, pages 1532–1543, 2014.
- [25] Alec Radford, Luke Metz, and Soumith Chintala. Unsupervised representation learning with deep convolutional generative adversarial networks. *arXiv preprint arXiv:1511.06434*, 2015.
- [26] Vignesh Ramanathan, Kevin Tang, Greg Mori, and Li Fei-Fei. Learning temporal embeddings for complex video analysis. In *Proceedings of the IEEE International Conference on Computer Vision*, pages 4471–4479, 2015.
- [27] D P Roy, M A Wulder, T R Loveland, C E Woodcock, R G Allen, M C Anderson, D Helder, J R Irons, D M Johnson, R Kennedy, T A Scambos, C B Schaaf, J R Schott, Y Sheng, E F Vermote, A S Belward, R Bindschadler, W B Cohen, F Gao, J D Hipple, P Hostert, J Huntington, C O Justice, A Kilic, V Kovalsky, Z P Lee, L Lyburner, J G Masek, J McCorkel, Y Shuai, R Trezza, J Vogelmann, R H Wynne, and Z Zhu. Landsat-8: Science and product vision for terrestrial global change research. *Remote Sensing of Environment*, 145(C):154–172, April 2014.
- [28] Aaron van den Oord, Nal Kalchbrenner, Lasse Espeholt, Oriol Vinyals, Alex Graves, et al. Conditional image generation with pixelcnn decoders. In *Advances in Neural Information Processing Systems*, pages 4790–4798, 2016.
- [29] Xiaolong Wang and Abhinav Gupta. Unsupervised learning of visual representations using videos. *arXiv preprint arXiv:1505.00687*, 2015.
- [30] Alyssa K Whitcraft, Eric F Vermote, Inbal Becker-Reshef, and Christopher O Justice. Cloud cover throughout the agricultural growing season: Impacts on passive optical earth observations. *Remote Sensing of Environment*, 156:438–447, January 2015.

A Experimental details

We use the scikit-learn random forest classifier implementation with 100 trees and default settings for all other parameters [23]. All neural network-based approaches including Tile2Vec are implemented in PyTorch and trained with the Adam optimizer with learning rate 0.001 and betas (0.5, 0.999). ResNet-18 models are trained with batch size 50. The convolutional autoencoder architecture has 3 convolutional layers and 2 linear layers in the encoder and 1 linear layer and 3 deconvolutional layers in the decoder; it is trained with batch size 100. Non-deep learning feature extraction approaches such as PCA, ICA, and k-means are fit on randomly sampled subsets of 10,000 points for tractability. Source code, trained models, and examples can be accessed at <https://github.com/ermongroup/tile2vec>.